Phys. Status Solidi B **247**, No. 8, 2075–2083 (2010) / **DOI** 10.1002/pssb.200983938

physica status solidi b
www.pss-b.com
basic solid state physics

Enhanced back and forward scattering in the reflection of light from weakly rough random metal surfaces

Ingve Simonsen*

Department of Physics, Norwegian University of Science and Technology (NTNU), NO-7491, Trondheim, Norway

Received 1 October 2009, revised 21 January 2010, accepted 22 February 2010
Published online 14 June 2010

Keywords light scattering, metal surfaces, surface plasmon polaritons

* Corresponding author: e-mail Ingve.Simonsen@ntnu.no, Phone: +47 73 59 34 17, Fax: +47 73 59 77 10

The scattering of light from a weakly rough random silver surface characterized by a double rectangular power spectrum is studied by numerical simulations. This power spectrum can support both the enhanced back and forward scattering phenomena, which for weakly rough surfaces, are both related to the excitation of surface plasmon polaritons. Here we review these phenomena and present new results from a numerical study of the dependence of the diffuse scattering on the amplitudes (γ_i, $i = 1, 2$) of the two rectangular portions of the power spectrum. It is found that there exist an optimal range of ratios, γ_2/γ_1, over which forward scattering peaks can be observed. By just changing the correlations along the interface, while keeping all other parameters like roughness, polarization, and angle of incidence unchanged, the fraction of the incident light that is scattered diffusely can be as large as 16%, while for other parameters as small as 1%. Moreover, a change in the correlation function only, can result in a 3.5 times increase in the amount of light that is absorbed at the weakly rough metal interface ($\sigma = 10$ nm).

1 Introduction Electromagnetic wave scattering from randomly rough surface has been a field of intensive research for more then a century [1–5]. During this time period significant progress has been made, but still open questions remains, in particular when it comes to dealing with effects of multiple scattering and two-dimensional surfaces. The continuous interest in this problem is not only due to the fundamental scientific issues involved, but is equally prompted by the wide range of applications that depends upon it. Such applications include radar and telecommunication technology, remote sensing, astrophysics, photovoltaics, medical applications, as well as more recently nanotechnology, and plasmonics.

A number of perturbative approaches has been developed for the scattering from randomly rough surface, and so have various computer simulation approaches [4]. Even if a formally exact solution to the two-dimensional scattering problem exists (in the form of integral equations), it is very computational demanding to utilize directly. However, for one-dimensional roughness, such rigorous computer simulation approaches can readily be used with confidence [4, 6] often without too much demand on computer time. With such techniques, the scattering from a number of systems has been studied: like, for instance, a single rough interface separating two semiinfinite media [4, 6], or film geometries where some or all of the interfaces are randomly rough [4, 7, 8]. This latter problem is, for instance, of importance in the design of effective solar cells [9]. Moreover, the scattering from fractal surfaces [10–12] and angular intensity correlation functions [4, 13] have also been studied. Even if the forward scattering problem, by far, is the most well studied, more recently the so-called inverse problem has also been approached [14–17]. Here one aims at predicting the (statistical) properties of the surface given some desired properties of the scattered field (e.g., angular distribution).

In the mid-1980s, McGurn et al. [18] predicted the existence of the enhanced backscattering phenomenon based on perturbation theory. This was the first unique *multiple scattering phenomenon* in the domain of rough surface scattering. Later this phenomenon was confirmed experientially for both weakly [19] and strongly rough surfaces [20]. Since the publication of Ref. [18], several other multiple scattering phenomena have been seen or predicted for rough surface scattering [4, 5].

The intention of this publication is to review some of these central coherent multiple scattering effects that can occur when light is being scattered from randomly rough surfaces, explain their physical origin, and to present some new results that can contribute to an even better understanding of them.

2 Scattering geometry The considered scattering system is depicted in Fig. 1, and consists of vacuum in the region $x_3 > \zeta(x_1)$, and a (non-magnetic) metal characterized by an isotropic, frequency-dependent, dielectric function $\varepsilon(\omega)$ in the region $x_3 < \zeta(x_1)$. We will assume that $\varepsilon(\omega)$ has a negative real part at the frequency, ω, of the incident light.

The surface profile function, $\zeta(x_1)$, is a single-valued function of x_1 and constitutes a zero-mean, stationary, Gaussian random process, that is differential with respect to its argument as many times as necessary. It is defined by

$$\langle \zeta^2(x_1) \rangle = \sigma^2, \tag{1a}$$

$$\langle \zeta(x_1)\zeta(x_1') \rangle = \sigma^2 W(|x_1 - x_1'|), \tag{1b}$$

where $W(|x_1|)$ denotes the (normalized) height–height correlation function of the surface roughness and σ is its root-mean-square (rms) value. The notation $\langle \cdot \rangle$ refers to taking an average of its argument over an ensemble of surface realizations.

3 Scattering theory For the geometry in Fig. 1, we will take the plane of incidence to be the x_1x_3-plane. When the incident field is p-polarized (s-polarized), it is convenient to work in terms of the single, non-zero component of the magnetic (electric) field that is perpendicular to the plane of incidence. To simplify the notation, we define

$$\Phi_\nu(x_1, x_3|\omega) = \begin{cases} H_2(x_1, x_3|\omega), & \nu = p, \\ E_2(x_1, x_3|\omega), & \nu = s, \end{cases} \tag{2}$$

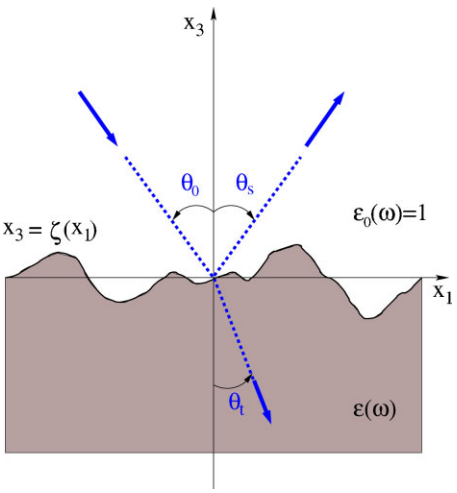

Figure 1 (online color at: www.pss-b.com) A sketch of the scattering geometry under study.

where the subscript ν denotes the polarization of the light. Note that for a one-dimensional scattering geometry, cross polarization is not possible (for the choice made for the plane of incidence). Once $\Phi_\nu(x_1, x_3|\omega)$ is known, the remaining two non-zero components of the electromagnetic field are readily obtained from the Maxwell's equations.

In the region $x_3 > \max \zeta(x_1)$, the field can be expressed as the sum of the incident and the scattered fields

$$\Phi_\nu^+(x_1, x_3|\omega) = \Phi_\nu^{\rm inc}(x_1, x_3|\omega) + \Phi_\nu^{\rm sc}(x_1, x_3|\omega). \tag{3}$$

For the incident field, we will for simplicity take a plane wave defined by

$$\Phi_\nu^{\rm inc}(x_1, x_3|\omega) = \Phi_0 e^{ikx_1 - i\alpha_0(k,\omega)x_3}, \tag{4}$$

where Φ_0 is a real *constant* amplitude (of appropriate physical units), k the wave vector component of the incident light that is parallel to the mean surface and related to the angle of incidence θ_0 via $k = (\omega/c)\sin\theta_0$, and where the perpendicular component is

$$\alpha_0(k,\omega) = \begin{cases} \sqrt{\frac{\omega^2}{c^2} - k^2}, & |k| < \frac{\omega}{c}, \\ i\sqrt{k^2 - \frac{\omega^2}{c^2}}, & |k| > \frac{\omega}{c}. \end{cases} \tag{5}$$

Due to the linearity of the Maxwell's equations, the scattered field can be written in the form

$$\Phi_\nu^{\rm sc}(x_1, x_3|\omega) = \Phi_0 \int_{-\infty}^{\infty} \frac{dq}{2\pi} R_\nu(q|k) e^{iqx_1 + i\alpha_0(q,\omega)x_3}, \tag{6}$$

where $R_\nu(q|k)$ represents the reflection amplitude of lateral wave vector of incidence, k, into light of lateral wave vector, q, scattered away from the interface. It is noted that the field in the form of Eq. (3), with Eqs. (4) and (6), automatically satisfies the boundary conditions at infinity.

Similarly, the field in the region $x_3 < \min \zeta(x_1)$ can be written

$$\Phi_\nu^-(x_1, x_3|\omega) = \Phi_0 \int_{-\infty}^{\infty} \frac{dq}{2\pi} T_\nu(q|k) e^{iqx_1 - i\alpha(q,\omega)x_3}, \tag{7}$$

where

$$\alpha(q,\omega) = \sqrt{\varepsilon(\omega)\frac{\omega^2}{c^2} - q^2}, \tag{8}$$

with $\mathrm{Re}\alpha(q,\omega) > 0$ and $\mathrm{Im}\alpha(q,\omega) > 0$.

3.1 Reduced rayleigh equation To proceed, it is required to known the reflection and/or transmission amplitudes, $R_\nu(q,\omega)$ and/or $T_\nu(q,\omega)$, appearing in Eqs. (6) and (7). To this end, we will adapt the method of the reduced Rayleigh equation, which is an approximative technique suitable of accurately describing the scattering from surfaces of not too steep slopes [21, 22]. We note that even if the approach is not rigorous, it is still a multiple scattering

technique. It consists of assuming that the asymptotic forms of the fields valid outside the surface region, Eqs. (6) and (7), can be used to satisfy the boundary conditions at the rough interface. This assumption is known as the *Rayleigh hypothesis* after Lord Rayleigh that used it to study the scattering from sinusoidal surfaces [1, 4, 5, 21].

From the general boundary conditions satisfied by any electromagnetic field at an interface [23, 24], it follows [4] that one should require both Φ_ν and $\partial_n \Phi_\nu / \kappa_\nu(\omega)$ to be continuous over the interface, where

$$\kappa_\nu(\omega) = \begin{cases} \varepsilon(\omega), & \nu = p, \\ \mu(\omega), & \nu = s. \end{cases} \tag{9}$$

Moreover, $\partial_n = \widehat{\mathbf{n}} \cdot \nabla$ denotes the normal derivative, where

$$\widehat{\mathbf{n}} = \frac{\zeta'(x_1)\widehat{\mathbf{x}}_1 + \widehat{\mathbf{x}}_3}{\sqrt{1 + (\zeta'(x_1))^2}} \tag{10}$$

is a unit normal vector to the surface (at point x_1) directed into vacuum. From these boundary conditions, one with Eqs. (6) and (7) is led to the following set of equations [4]

$$\begin{aligned} &\mathrm{e}^{ikx_1 - i\alpha_0(k,\omega)\zeta(x_1)} + \int \frac{\mathrm{d}q}{2\pi} R_\nu(q|k) \mathrm{e}^{iqx_1 + i\alpha_0(q,\omega)\zeta(x_1)} \\ &\quad = \int \frac{\mathrm{d}q}{2\pi} T_\nu(q|k) \mathrm{e}^{iqx_1 - i\alpha(q,\omega)\zeta(x_1)} \end{aligned} \tag{11a}$$

and

$$\begin{aligned} &\int \frac{\mathrm{d}q}{2\pi} \mathrm{e}^{iqx_1} \Big[-2\pi\delta(q-k)\{\zeta'(x_1)q + \alpha_0(q,\omega)\} \\ &\qquad \times \mathrm{e}^{-i\alpha_0(q,\omega)\zeta(x_1)} \\ &\qquad + R_\nu(q|k)\{-\zeta'(x_1)q + \alpha_0(q,\omega)\} e^{i\alpha_0(q,\omega)\zeta(x_1)} \Big] \\ &\quad = -\kappa_\nu(\omega) \int \frac{\mathrm{d}q}{2\pi} \mathrm{e}^{iqx_1} T_\nu(q|k)\{\zeta'(x_1)q + \alpha(q,\omega)\} \\ &\qquad \times \mathrm{e}^{-i\alpha(q,\omega)\zeta(x_1)}. \end{aligned} \tag{11b}$$

Equations (11) represent a set of two coupled integral equations known as the *Rayleigh equations*. However, they can be reduced to one single integral equation for either the reflection or transmission amplitude, and here $T_\nu(q,\omega)$ will be eliminated since no (deep) transmission into the metal is possible. On multiplying Eq. (11a) by $\mathrm{e}^{-ipx_1 - i\alpha(p,\omega)\zeta(x_1)}[-\zeta'(x_1)p + \alpha(p,\omega)]$, Eq. (11b) by $\kappa_\nu \mathrm{e}^{-ipx_1 - i\alpha(p,\omega)\zeta(x_1)}$, adding the two equations and integrating the result over x_1, one, after some algebra, arrives at

$$\int_{-\infty}^{\infty} \frac{\mathrm{d}q}{2\pi} M_\nu^+(p|q) R_\nu(q|k) = M_\nu^-(p|k), \tag{12a}$$

where

$$\begin{aligned} M_\nu^\pm(p|q) = &\pm I(\alpha(p,\omega) \mp \alpha_0(q,\omega)|p-q) \\ &\times \Big[\frac{(p + \kappa_\nu(\omega)q)(p-q)}{\alpha(p,\omega) \mp \alpha_0(q,\omega)} \\ &+ \alpha(p,\omega) \pm \kappa_\nu(\omega)\alpha_0(q,\omega) \Big] \end{aligned} \tag{12b}$$

and where $I(\gamma|q)$ is an integral defined as

$$I(\gamma|q) = \int_{-\infty}^{\infty} \mathrm{d}x_1 \mathrm{e}^{-i\gamma\zeta(x_1)} \mathrm{e}^{-iqx_1}. \tag{12c}$$

Equations (12) represent a single integral equation for the reflection amplitude, known as the *reduced Rayleigh equation* [4]. It forms the starting point for most, if not all, perturbative approaches to rough surface scattering [4]. Moreover, Eqs. (12) have also be used successfully as basis for direct numerical simulations [25, 26].

3.2 Mean differential reflection coefficient The physical observable quantity that we will be concerned with in this work, is the so-called mean differential reflection coefficient (DRC), $\langle \partial R_\nu / \partial \theta_\mathrm{s} \rangle$. It is defined as the fraction of the power flux incident on the rough surface that is scattered by it into an angular interval of width $\mathrm{d}\theta_\mathrm{s}$ about the scattering angle θ_s.

The power flux incident on the surface is calculated from the real part of the 3-component of the time averaged (complex) Poynting vector $\langle \mathbf{S} \rangle_t = (1/2)\mathbf{E} \times \mathbf{H}^*$, integrated over a plane parallel to $x_3 = 0$, where the notation $\langle \cdot \rangle_t$ denotes time-averaging. In this way and with Eq. (4), one obtains

$$P_\mathrm{inc} = \frac{L_1 L_2}{2} \frac{\Phi_0^2}{\xi_\nu} \cos\theta_0, \tag{13}$$

where L_1 and L_2 are the lengths of the surface along the x_1 and x_2 directions, respectively, and $\xi_p = 1/\eta_\circ$ and $\xi_s = \eta_\circ$ with $\eta_\circ = \sqrt{\mu_\circ/\varepsilon_\circ}$ being the free-space impedance. In a similar way, by using Eq. (6), it is obtained that the power flux scattered by the surface is

$$P_\mathrm{sc} = \int_{-\frac{\pi}{2}}^{\frac{\pi}{2}} \mathrm{d}\theta_\mathrm{s} p_\mathrm{sc}(\theta_\mathrm{s}), \tag{14a}$$

where

$$p_\mathrm{sc}(\theta_\mathrm{s}) = \frac{L_2}{4\pi} \frac{\Phi_0^2}{\xi_\nu} \frac{\omega}{c} \cos^2\theta_\mathrm{s} |R_\nu(q|k)|^2. \tag{14b}$$

According to its definition and with Eqs. (13) and (14), the mean DRC can be written as

$$\begin{aligned} \left\langle \frac{\partial R_\nu}{\partial \theta_\mathrm{s}} \right\rangle &= \left\langle \frac{p_\mathrm{sc}(\theta_\mathrm{s})}{P_\mathrm{inc}} \right\rangle \\ &= \frac{1}{L_1} \frac{\omega}{2\pi c} \frac{\cos^2\theta_\mathrm{s}}{\cos\theta_0} \left\langle |R_\nu(q|k)|^2 \right\rangle. \end{aligned} \tag{15}$$

Rewriting this expression enables us to identify two contributions to the mean DRC – the *coherent* (specular) and *incoherent* (diffuse) components. These two contributions, which sum is given by Eq. (15), are respectively:

$$\left\langle \frac{\partial R_\nu}{\partial \theta_s} \right\rangle_{\rm coh} = \frac{1}{L_1} \frac{\omega}{2\pi c} \frac{\cos^2\theta_s}{\cos\theta_0} |\langle R_\nu(q|k)\rangle|^2 \tag{16a}$$

and

$$\left\langle \frac{\partial R_\nu}{\partial \theta_s} \right\rangle_{\rm incoh} = \frac{1}{L_1} \frac{\omega}{2\pi c} \frac{\cos^2\theta_s}{\cos\theta_0} \times \left[\left\langle |R_\nu(q|k)|^2 \right\rangle - |\langle R_\nu(q|k)\rangle|^2 \right]. \tag{16b}$$

In Eqs. (15) and (16), k and q are understood to be related to the angles of incidence (θ_0) and scattering (θ_s) via

$$k = \frac{\omega}{c}\sin\theta_0, \quad q = \frac{\omega}{c}\sin\theta_s. \tag{17}$$

For later use, we also define the quantity

$$\mathcal{U}_\nu(\theta_0) = \int_{-\pi/2}^{\pi/2} {\rm d}\theta_s \left\langle \frac{\partial R_\nu}{\partial \theta_s} \right\rangle. \tag{18}$$

It is interpreted as the fraction of the power flux of the incident light that is scattered away from the rough surface irrespectively of scattering angle. If there is no absorption in the metal, energy conservation requires that $\mathcal{U}_\nu(\theta_0) = 1$ (for all θ_0). However, for real metals, $\mathcal{U}_\nu(\theta_0) < 1$ due to absorption. Note, that $\mathcal{U}_\nu(\theta_0)$, like $\langle \partial R_\nu/\partial\theta_s\rangle$, can be separated into a coherent and an incoherent contribution.

3.3 Power spectrum In the discussion to follow, the power spectrum of the surface roughness will be important. It is defined as the Fourier transform of the (normalized) correlations function

$$g(|k|) = \int_{-\infty}^{\infty} {\rm d}x_1 W(|x_1|) {\rm e}^{-ikx_1}. \tag{19}$$

The form of the power spectrum that will be the main focus of this work is the rectangular form that takes on a non-zero and constant value *only* inside the interval $k_- < |k| < k_+$.

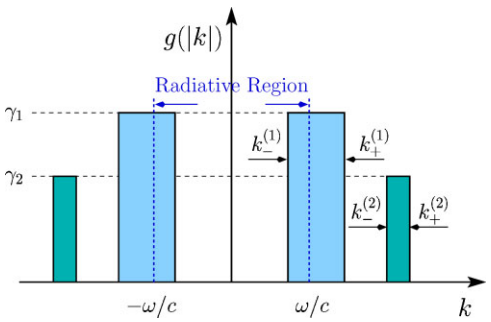

Figure 2 (online color at: www.pss-b.com) A sketch of the power spectrum, Eq. (20), used in this work.

Roughness showing this type of power spectrum was recently proposed, manufactured, and used in a nice experimental study of the enhanced backscattering phenomenon from weakly rough surfaces [27].

In this work we will be even more general and allow for two such non-zero intervals for $k > 0$. We define (see Fig. 2)

$$g(|k|) = \gamma_1 g_1(|k|) + \gamma_2 g_2(|k|), \tag{20a}$$

with

$$g_i(|k|) = \frac{\pi}{k_+^{(i)} - k_-^{(i)}} \left[H(k_+^{(i)} - k) H(k - k_-^{(i)}) + H(k_+^{(i)} + k) H(-k - k_-^{(i)}) \right], \tag{20b}$$

where $\gamma_i \geq 0$ ($i = 1,2$) are constants so that $\gamma_1 + \gamma_2 = 1$ and $H(\cdot)$ denotes the Heaviside step function.

3.4 Small amplitude perturbation theory One of the earliest perturbative approaches to rough surface scattering, was the *small amplitude perturbation theory* [4], which is appropriate if the surface roughness, σ, is sufficiently smaller than the wavelength of the incident light. This method amounts to expanding the reflection amplitude in the series $R_\nu(q|k) = \sum_{n=0}^{\infty} R_\nu^{(n)}(q|k)/n!$, where $R_\nu^{(n)}(q|k)$ is of order $O(\zeta^n)$ in the surface profile function $\zeta(x_1)$ [4]. Substituting this expansion into the reduced Rayleigh equation, Eq. (12a) and Taylor expanding Eq. (12c), it follows readily that the lowest order contribution to the incoherent component of the mean DRC can be written in the form [4]

$$R_\nu(q|k) = 2\pi\delta(q-k) r_\nu(k) + \chi_\nu(q|k)\tilde{\zeta}(q-k) + \mathcal{O}(\tilde{\zeta}^2),$$

where $r_\nu(k)$ is the Fresnel reflection amplitude, $\tilde{\zeta}(q)$ is the Fourier transform of the surface roughness $\zeta(x_1)$, and $\chi_\nu(q|k)$ is a function independent of the surface roughness that will not be important for the following discussion (for details, see Ref. [4]). With this expression, it follows from Eq. (16b) that the lowest order (single scattering) contribution to the incoherent component of the mean DRC is

$$\left\langle \frac{\partial R_\nu}{\partial \theta_s} \right\rangle_{\rm incoh} \propto g(|q-k|). \tag{21}$$

Moreover, the leading term in the contribution to the coherent component of $\langle \partial R_\nu/\partial\theta_s\rangle$ will be proportional to the Fresnel reflection coefficient $|r_\nu(k)|^2$ [4, 5].

3.5 Surface plasmon polaritons Surface plasmon polaritons (SPPs) are surface electromagnetic waves that can propagate along a dielectric-metal interface [4, 5, 28]. By imposing the boundary conditions satisfied by the field, it is readily shown that such modes can only exist in p-polarization and when the two media have opposite signs for the real parts of their dielectric functions. Moreover, their

(lateral) wave vector is given by [4, 28]

$$k_{\rm spp}(\omega) = \frac{\omega}{c}{\rm Re}\sqrt{\frac{\varepsilon(\omega)}{\varepsilon(\omega)+1}}. \qquad (22)$$

Since $k_{\rm spp} > \omega/c$, we note that the SPPs are evanescent (non-radiating) in both the dielectric and in the metal, and, hence, light incident on a flat dielectric-metal interface *cannot* excite SPPs due to the (lateral) wave vector mismatch. On the other hand, if the surface is rough, such waves can be excited with a coupling strength proportional to $g(|\pm k_{\rm spp} - k|)$ as explained in the preceding subsection.

4 Results We have conducted numerical simulations based on the reduced Rayleigh equation, Eq. (12), for the vacuum-silver system described in Section 2. In these simulations, it has been assumed that the wavelength of the incident light is $\lambda = 457.9$ nm (in vacuum) at which wavelength the dielectric function of silver is $\varepsilon(\omega) = -7.5 + 0.24i$ [29]. With this value for $\varepsilon(\omega)$, Eq. (22) predicts that $k_{\rm spp}(\omega) = 1.074\omega/c$ for the SPP supported by the system. The length of the surface along the x_1 direction was taken to be $L_1 = 200\lambda$, and it was discretized with 28.62 points per wavelength corresponding to a sampling interval of $\Delta x_1/\lambda = 0.035$. The rough surface was characterized by an rms roughness of $\sigma = 10$ nm and a power spectrum in the form of Eq. (20) with parameters: $k_-^{(1)} = 0.782\omega/c$, $k_+^{(1)} = 1.366\,\omega/c$, $k_-^{(2)} = 2.048\,\omega/c$, and $k_+^{(2)} = 2.248\,\omega/c$, for which $k_{\rm spp} \in [k_-^{(1)}, k_+^{(1)}]$ and $2k_{\rm spp} \in [k_-^{(2)}, k_+^{(2)}]$. These values for $k_\pm^{(1)}$ and $k_\pm^{(2)}$ are identical to those used in the recent study by O'Donnell and Mendez [30].

We are about to present the results of a systematic study of how the scattering depends on the power spectrum amplitudes γ_1 and γ_2. In contrast to what was done in Ref. [30], the rms roughness of the surface, σ, will here remain fixed as we change the ratio γ_2/γ_1. Hence it is only the correlation along the surface that is influenced by changing the ratio γ_2/γ_1.

4.1 Backscattering enhancement Initially we investigate and review the diffuse scattering from surfaces characterized by only one of the two components of the power spectrum, i.e., when γ_2/γ_1 is 0 or ∞. In Figs. 3, we present simulation results for the incoherent (diffuse) component of the mean DRC for p-polarized plane waves incident on the surface at an angle of incidence θ_0 and where the total power spectrum of the surface roughness was equal to either $g_1(|k|)$ (Fig. 3a) or $g_2(|k|)$ (Fig. 3b). Striking differences are observed between the scattering patterns in the two cases. Even if these dependencies today are fairly well understood, the arguments leading to their explanation will for completeness be repeated here.

The situation where $\gamma_2 = 0$ will be considered first (Fig. 3a). The most apparent features of Fig. 3a are the pronounced peaks located at scattering angles $\theta_{\rm s} = -\theta_0$. This is the *enhanced backscattering phenomenon* first predicted theoretically for the scattering from weakly rough surfaces

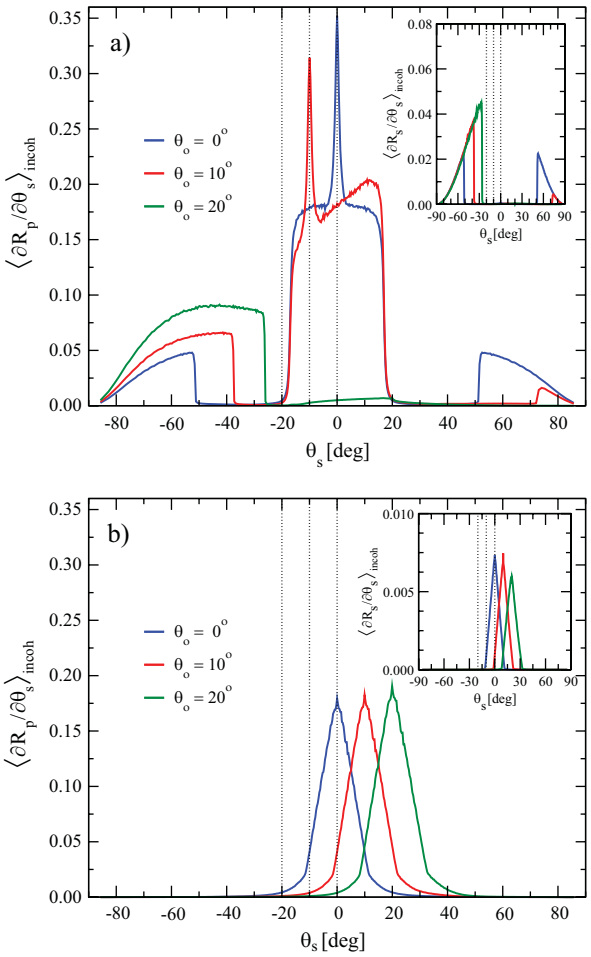

Figure 3 (online color at: www.pss-b.com) The incoherent component of the mean DRC, $\langle \partial R_v/\partial\theta_{\rm s}\rangle_{\rm incoh}$, for an either p- (main panel) or s-polarized plane wave (inset) incident from vacuum on a rough silver surface at wavelength $\lambda = 457.9$ nm ($\varepsilon(\omega) = -7.5 + 0.24i$) and an angle of incidence θ_0 as given by the legends. The rough surface (of length $L = 200\lambda$) had a Gaussian height distribution of rms-height 10 nm, and the power spectrum was characterized by Eq. (20) with $k_-^{(1)} = 0.782\omega/c$, $k_+^{(1)} = 1.366\,\omega/c$, $k_-^{(2)} = 2.048\,\omega/c$, and $k_+^{(2)} = 2.248\,\omega/c$, with either (a) $\gamma_1 = 1$ and $\gamma_2 = 0$ or (b) $\gamma_1 = 0$ and $\gamma_2 = 1$. The vertical dotted lines indicate the backscattering directions. The results were averaged over 10,000 realizations of the surface roughness. For p-polarized light, incident at an angle $|\theta_0| < \theta_{\rm max} = 17°$, the enhanced backscattering peaks are readily observed in the diffusely scattered light.

[18], but, however, observed experimentally first for strongly rough surfaces [20] and some years later for surfaces that are weakly rough [19]. For weakly rough metallic surfaces this phenomenon is only seen in p-polarization, while for s-polarization it is not present (see Fig. 3a, inset). However, for strongly rough surfaces it is observed for both polarizations [20] – also for non-metallic surfaces – and it is in this case ascribed to constructive interference of volume waves scattered multiple times by the roughness, but in *reversed order* [20]. But what is causing the phenomenon in the case of weakly rough surfaces? The authors of Refs. [18, 19]

attributed it to the multiple scattering and constructive interference of scattering sequences containing SPPs (or other surface waves) as an intermediate state. This explains why enhanced backscattering is only observed for weakly rough surfaces in p-polarization (Fig. 3a), since only for this polarization can SPPs be excited by the incident light. To lowest order, the relevant sequences involved are: $k \to \pm k_{\rm spp}(\omega) \to -k$, and these two processes, when scattered from the same points on the surface, but in opposite order, will have zero phase difference and, therefore, interfere constructively. If the complex amplitudes of the two processes are denoted as $\mathcal{A}e^{i\phi_i}$, where their (real-valued) amplitudes have been assumed to be equal, for simplicity, their contribution to the intensity in the backscattering direction will be [4] $I_{1+2} = \langle |\mathcal{A}e^{i\phi_1} + \mathcal{A}e^{i\phi_2}|^2 \rangle = 4I$ with $I = \mathcal{A}^2$ (since $\phi_1 = \phi_2$). However, away from the backscattering direction, the phase difference $\phi_2 - \phi_1$ will be a random function since it will depend on the surface roughness, $\zeta(x_1)$. Hence the interference term will average to zero, $\langle e^{i(\phi_2 - \phi_1)} \rangle = 0$, so that in this case $I_{1+2} = 2I$. Thus, the backscattering peak should rise twice over the background if single scattering does not contribute to the scattered intensity for angles of scattering around $\theta_s = -\theta_0$. This is precisely what is observed in Fig. 3a, since below we will see that single scattering gives no contribution to the scattered light over an angular interval containing the backscattering direction.

From Fig. 3a one observes that the enhanced backscattering peaks do not exist for all angles of incidence, e.g., $\theta_0 = 20^\circ$. For the above SPP mediated multiple scattering process to take place, it must be possible for the incident light, of lateral wave vector $k = (\omega/c)\sin\theta_0$, to couple into rightward (+) and/or leftward-propagating (−) SPPs of wave vectors $\pm k_{\rm spp}(\omega)$. From the discussion in Section 3 it follows that this is only possible if $g(|\pm k_{\rm spp}(\omega) - k|) \neq 0$, or if the angle of incidence (θ_0) is smaller in absolute value than the *critical* angle

$$\theta_{\max} = \sin^{-1}\left(\frac{k_{\rm spp}(\omega) - k_-^{(1)}}{\omega/c}\right). \tag{23}$$

Furthermore, it is straightforwardly shown that only for $|\theta_s| < \theta_{\max}$ is out-coupling of SPPs into propagating waves possible. With the parameters assumed in the simulations, one finds $\theta_{\max} = 17^\circ$, and this is the reason why no enhanced backscattering peak is seen in Fig. 3a when $\theta_0 = 20^\circ$. Moreover, the explanation for the rapid drop in intensity of p-polarized scattered light just outside $\theta_s = \pm\theta_{\max}$, is that here out-coupling of SPPs into propagating modes is forbidden. For s-polarization, for which SPPs cannot be excited, there is nothing special about the scattering angles around $\pm\theta_{\max}$ (and the mean DRC is smooth).

Figure 3a also shows pronounced increase in the values of $\langle \partial R_p/\partial\theta_s \rangle_{\rm incoh}$ for some (large) scattering angles in the range $|\theta_s| > \theta_{\max}$ (for $\theta_0 = 10^\circ$ located at $\theta_s = \pm 51.4^\circ$). This has nothing to do with SPPs, nor with multiple scattering, but is instead an effect of single scattering (and the actual power spectrum parameters used). According to Eq. (21), incident light of lateral wave vector k can, by single scattering only, be coupled to propagating scattered light of lateral wave vector q, if $g(|q-k|)$ is non-zero. With the power spectrum assumed here this is possible when $|q-k| > k_-^{(1)}$. For instance, when the angle of incidence is $\theta_0 = 10^\circ$, the above relation predicts that single scattering is allowed for angles of scattering for which $\theta_s > 72.8^\circ$ and $\theta_s < 37.4^\circ$. Conversely, in the interval $-37.4^\circ < \theta_s < 72.8^\circ$ single scattering is *forbidden* due to the form (and parameters) of the power spectrum. From Fig. 3a, it is observed that it is just outside this angular interval (when $\theta_0 = 10^\circ$) that the sudden increase in $\langle \partial R_p/\partial\theta_s \rangle_{\rm incoh}$ takes place. Arguments similar to those just given do also apply for other angles of incidence, but will not be presented here.

The situation where the power spectrum parameters are $\gamma_1 = 0$ and $\gamma_2 = 1$ (with all other parameters unchanged) is presented in Fig. 3b. In this case SPPs can no longer be excited by the incident light for any angles of incidence, and single scattering is forbidden for all scattering angles $-90^\circ < \theta_s < 90^\circ$. Instead the incident light can excite numerous non-resonant evanescent modes (of lateral wave vectors p with $|p| \in [k_-^{(2)}, k_+^{(2)}]$) that are scattered *multiple times* by the surface roughness before being converted into propagating modes scattered away from the interface. This results in an angular distribution of the diffusely scattered light that is very different from that when SPPs can be excited. Moreover, the distribution of the scattered light is more "traditional" in the sense that it is almost symmetrically distributed around the specular direction, $\theta_s = \theta_0$, and drops off in intensity as the angular distance from the specular direction increase. These distributions will not be discussed further here, but we note that in this case the diffuse scattering is rather similar for both p- and s-polarization (Fig. 3 and its insets). In particular, note from Fig. 3b that nothing "dramatic" happens to the scattering distributions when the angle of incidence is increased above $\theta_0 = \theta_{\max}$.

4.2 Forward scattering enhancement We studied the situation where neither γ_1 nor γ_2 is zero, i.e., the power spectrum $g(|k|)$ receives contributions from both $g_1(|k|)$ and $g_2(|k|)$. Numerical simulation results for this situation are presented in Figs. 4 for a set of values of the ratio γ_2/γ_1 distributed over the range $[0, \infty)$. For all cases, the light incident on the surface was p-polarized, and the angle of incidence was $\theta_0 = 10^\circ$. We recall that changing γ_2/γ_1 does not influence the rms roughness of the surface and it was therefore constant (and equal to $\sigma = 10$ nm) for all cases.

There are several interesting features to be observed from Figs. 4. Those that will be focused on here are: (i) the peak structure of the diffuse component of the mean DRC, and (ii) how the amount of diffusely scattered light depends on the ratio γ_2/γ_1.

From Fig. 4a it is apparent that increasing γ_2/γ_1 (from zero) will gradually lead to the appearance of peaks at the specular direction, $\theta_s = \theta_0$, in addition to the backscattering peaks already existing at $\theta_s = -\theta_0$. However, when γ_2 is

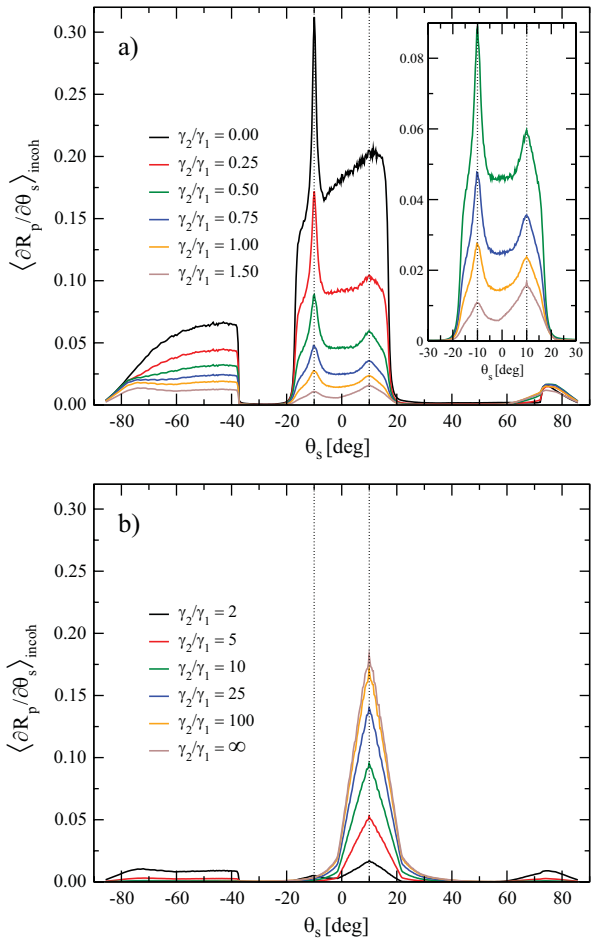

Figure 4 (online color at: www.pss-b.com) The same as Fig. 3, but now for a fixed angle of incidence $\theta_0 = 10^\circ$ and for different values of the power spectrum amplitude ratio γ_2/γ_1. When this ratio is different from zero, and $\gamma_2/\gamma_1 \sim 1$ enhanced forward scattering peaks start to be observed in addition to the backscattering peaks. The dotted vertical lines indicate the position of the forward scattering (specular) and backscattering directions.

becoming significantly larger than γ_1, the backscattering peak disappears, and a "Λ-shaped" intensity distribution of the scattered light is instead emerging (Fig. 4b). The intensities of the maxima of these latter distributions, located at the specular positions, are increasing with γ_2/γ_1 while their baseline widths seem to be less affected by the same ratio. In this latter case, as the angle of incidence is changed to above θ_{max} (results not shown), no dramatic effect on the scattering pattern is observed (except for an angular translation), indicating that SPPs are not contributing significantly to the scattering. However, for moderate values of the ratio γ_2/γ_1, and for which also backscattering peaks are observed (Fig. 4a), a marked change in the scattering patterns is observed as the angle of incidence is increased from below to above θ_{max} (Fig. 5). Recalling that the coupling constants of the incident light into SPPs essentially is γ_1, the above observations is to be expected.

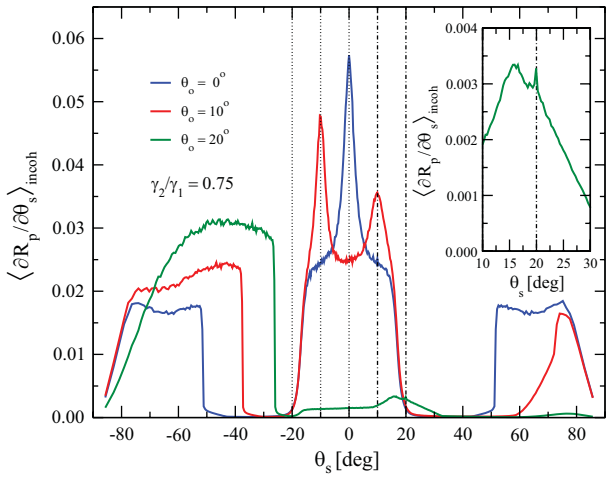

Figure 5 (online color at: www.pss-b.com) Same as Fig. 3a, but for $\gamma_2/\gamma_1 = 0.75$. The vertical dash-dotted lines indicate the forward scattering (specular) directions. The inset shows a close-up of the curve corresponding to $\theta_0 = 20^\circ$. It shows that forward scattering peaks are in principle also possible if SPPs cannot be excited by the incident light, but in this case the phenomenon is much less pronounced.

The physical origin of the peaks at $\theta_s = \theta_0$ was first reported and discussed by O'Donnell [31] based on a high-order perturbation theory (4th order). It was here shown that the existence of these peaks required a power spectrum that supports the *counter-propagation* of SPPs.[1] By counter-propagating SPPs, we mean the scattering processes where an SPP propagating in one direction being scattered by the surface roughness into another SPP that is propagating in the opposite direction; $\pm k_{spp}(\omega) \rightarrow \mp k_{spp}(\omega)$. Such processes are only possible if $g(2k_{spp}) \neq 0$ at the frequency, ω, of the incident radiation. O'Donnell [31] coined the term "enhanced specular peaks" for the phenomenon due to the angular position of these peaks. However, it has nothing to do with specular scattering, and for that reason, we suggest the alternative name "*enhanced forward scattering peaks*", in order to avoid any confusion.

Moreover, O'Donnell [31] demonstrated that the lowest order terms in perturbation theory contributing to the enhanced forward scattering phenomenon consist of a set of fourth order scattering process that can interfere constructively only in the forward direction $\theta_s = \theta_0$. One of the contributing scattering sequences is, $k \rightarrow -k_{spp} \rightarrow k_{spp} \rightarrow -k_{spp} \rightarrow k$ that includes, as stated above, the counter-propagation of SPPs [31]. For a detailed technical discussion of the involved scattering processes we refer the interested reader to the original literature [30, 31]. Here it suffices to stress that if $g(2k_{spp}) = 0$, then the enhanced forward scattering peaks essentially disappear (Fig. 4a). However,

[1] As long as the power spectrum supports counter-propagation, forward scattering peaks should in principle be possible. However, only when resonant modes can be excited, like SPPs, will the phenomenon be pronounced (Fig. 5).

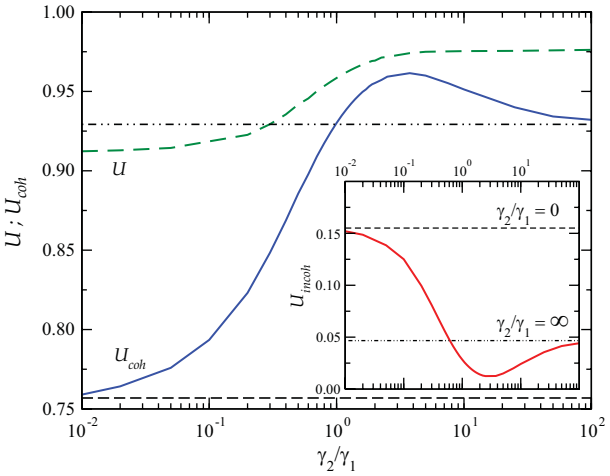

Figure 6 (online color at: www.pss-b.com) The fraction of the incident power flux that is reflected by the surface, $\mathcal{U}$, and its coherent and incoherent components, $\mathcal{U}_{\rm coh}$ and $\mathcal{U}_{\rm incoh}$, respectively, as a function of the power spectrum amplitude ratio γ_2/γ_1. The angle of incidence of the p-polarized light used to obtain these results was $\theta_0 = 10^\circ$, while the remaining parameters were as given in the caption of Fig. 3.

$g(2k_{\rm spp}) \neq 0$ does not guarantee that forward scattering peaks can be observed, since also the coupling of the incident light into SPPs must be strong for this to happen (see Fig. 4b). In passing it is noted that the level of surfaces roughness considered here is well above what practically can be approached by perturbation theory, so higher order scattering sequences to those indicated above will likely contribute significantly to the peaks at $\theta_{\rm s} = \theta_0$ [30].

Fig. 4a clearly demonstrates that the amount of light scattered diffusely by the surface depends strongly on the power spectrum amplitude ratio γ_2/γ_1, or, equivalently, on the correlations along the surface. To investigate and quantify this behavior further, Fig. 6, for $\theta_0 = 10^\circ$, presents numerical simulation results for $\mathcal{U}(\theta_0)$ as well as its coherent and incoherent components. It is found that as γ_2/γ_1 is increased from 0 to ∞, $\mathcal{U}(\theta_0)$ will increase monotonously from 0.911 to 0.976. So by changing only the surface height correlation function, but keeping the surface height distribution unchanged, we can increase the amount of absorption in the silver by almost 8%, and this for a weakly rough surface. Moreover, it is observed from Fig. 6, that neither $\mathcal{U}_{\rm coh}$ nor $\mathcal{U}_{\rm incoh}$ is monotonous functions of γ_2/γ_1, but show instead increasing and decreasing behaviors. Their extreme points are for $\theta_0 = 10^\circ$ found close to $\gamma_2/\gamma_1 \approx 3$ for which $\mathcal{U}_{\rm coh}$ is at its maximum and $\mathcal{U}_{\rm incoh}$ at its minimum. Other values for the angle of incidence gave qualitatively similar behavior for $\mathcal{U}(\theta_0)$ as long as the incident light could couple to SPPs, i.e., for $|\theta_0| \leq \theta_{\rm max}$.

How can the behavior seen in Fig. 6 be rationalized? The strongest absorption is expected when SPPs are excited strongly since these modes can propagate long distances along the vacuum-silver interface while energy continuously is converted to heat in the metal. Whenever, γ_2/γ_1 is small, the coupling into SPPs is at its most efficient (if $|\theta_0| \leq \theta_{\rm max}$), and as γ_2 is increased, the coupling of the incident light into SPPs is reduced, and less light is therefore absorbed. Similarly, the amount of light undertaking single scattering (allowed for the largest scattering angles) will decrease with increasing γ_2 (Fig. 4a). Based on such simple arguments, it is to be expected that the amount of scattered energy, $\mathcal{U}(\theta_0)$, should increase with increasing γ_2/γ_1, and this dependence is indeed also what is observed from Fig. 6.

Once an SPP is excited, it can couple out into radiative modes that propagate away for the surface over a range of scattering angles ($|\theta_{\rm s}| < \theta_{\rm max}$). This scattered light will therefore contribute mainly to $\mathcal{U}_{\rm incoh}$, and is the reason why one from Fig. 6 observes increasing (decreasing) values for $\mathcal{U}_{\rm coh}$ ($\mathcal{U}_{\rm incoh}$) when γ_2/γ_1 is increased from zero. However, for some value of γ_2/γ_1, γ_1 is small enough for the coupling into SPPs or single scattered light not to be very efficient, and, at the same time, γ_2 is not large enough for the multiple scattering of the non-resonant evanescent modes to be very significant. This situation results in a local minimum (maximum) in $\mathcal{U}_{\rm incoh}$ ($\mathcal{U}_{\rm coh}$) that for $\theta_0 = 10^\circ$ is located at $\gamma_2/\gamma_1 \approx 3$ (Fig. 6). As γ_2/γ_1 is increased even further, the coupling into SPPs is essentially no longer possible and neither is single scattering (since $\gamma_1 \approx 0$). However, due to increasing γ_2, an increase in the evanescent non-resonant multiple scattering will take place resulting in the observed increase in $\mathcal{U}_{\rm incoh}$. This argument alone, however, does not explain why $\mathcal{U}(\theta_0)$ is flat (and not dropping) in this region, something we speculate is due to the short propagating length of the non-resonant evanescent modes.

5 Conclusions In conclusion, we have studied by numerical simulations the scattering of light from weakly rough silver surfaces characterized by a double rectangular power spectrum. Such power spectra support both the classic enhanced backscattering phenomena, but also the more recent forward scattering enhancement phenomenon. Both are for weakly rough surfaces intimately related to the excitation of SPPs, and the latter does require that such surface modes can counter propagate. We have reviewed and explained in detail both of these phenomena. Moreover, new numerical results were presented for the dependence of the diffusely scattered light on the amplitudes of the two rectangular portions of the power spectrum (γ_1 and γ_2). It was demonstrated that an optimal range of ratios γ_2/γ_1 exists over which the forward scattering peak phenomenon can be observed. By just changing the correlations along the interface, while keeping all other parameters like roughness, polarization, and angle of incidence unchanged, the amount of light that is absorbed by the weakly rough silver surface ($\sigma = 10$ nm) can be increased more than three times. Moreover, under the same conditions, a change in the portion of the incident light that is scattered diffusely can vary by a factor close to 15.

Acknowledgements The author would like to thank Department of Physics and Astronomy, University of California, Irvine for kind hospitality during the time that this work was

conducted. It is also a pleasure to acknowledge Dr. Tamara A. Leskova and Dr. Alexei A. Maradudin for fruitful and inspiring discussions. This research was supported in part by the Research Council of Norway under the program Småforsk and an NTNU mobility grant.

References

[1] L. Rayleigh, The Theory of Sound (Dover Publications, New York, 1945).
[2] A. G. Voronovich, Wave Scattering From Rough Surfaces (Springer Verlag, New York, 1994).
[3] A. A. Maradudin (ed.), Light Scattering and Nanoscale Surface Roughness (Springer Verlag, New York, 2007).
[4] I. Simonsen, Optics of surface disordered systems: A random walk through surface scattering phenomena, 2009, accepted for publication in Eur. Phys. J. Special Topics (arXiv:cond-mat/0408017).
[5] A. Shchegrov, A.A. Maradudin, and E.R. Méndez, Prog. Opt. **46**, 117 (2004).
[6] A.A. Maradudin, T. Michel, A.R. McGurn, and E.R. Méndez, Ann. Phys. **203**, 255 (1990).
[7] I. Simonsen and A. Maradudin, Opt. Commun. **162**, 99 (1999).
[8] A. Soubret, G. Berginc, and C. Bourrely, Phys. Rev. B **63** 24 245411 (2001).
[9] S. Fahr, C. Rockstuhl, and F. Lederer, Appl. Phys. Lett. **92**, 171114 (2008).
[10] I. Simonsen, D. Vandembroucq, and S. Roux, Phys. Rev. E **61**, 5914 (2000).
[11] I. Simonsen, D. Vandembroucq, and S. Roux, J. Opt. Soc. Am. A **18**, 1101 (2001).
[12] I. Simonsen, A. Tarrats, and D. Vandembroucq, J. Opt. A, Pure Appl. Opt. **4**, S168 (2002).
[13] T. Leskova, I. Simonsen, and A.A. Maradudin, Waves Random Media **12**, 307 (2002).
[14] A. Maradudin, T. Leskova, and E. Méndez, Designer Surfaces (Elsevier, Amsterdam, 2008).
[15] E. R. Méndez, E.E. García-Guerrero, T. A. Leskova, A. A. Maradudin, J. Muñoz-López, and I. Simonsen, Appl. Phys. Lett. **81**, 798 (2002).
[16] A. Maradudin, I. Simonsen, T. Leskova, and E. Méndez, Waves Random Media **11**, 529 (2001).
[17] A. Maradudin, I. Simonsen, T. Leskova, and E. R. Méndez, Opt. Lett. **24**, 1257 (1999).
[18] A.R. McGurn, A.A. Maradudin, and V. Celli, Phys. Rev. B **31**, 4866–4871 (1985).
[19] C. West and K. O'Donnell, J. Opt. Soc. Am. A **12**, 390 (1995).
[20] E. Méndez and K. O'Donnell, Opt. Commun. **61**, 91 (1987).
[21] T. Watanabe, Y. Choyal, K. Minami, and V. Granatstein, Phys. Rev. E **69**, 056606 (2004).
[22] A.V. Tishchenko, Opt. Express **17**, 17102 (2009).
[23] J. Stratton, Electromagnetic Theory, IEEE Press Series on Electromagnetic Wave Theory (Wiley-IEEE Press, New York, 2007).
[24] J. Jackson, Classical Electrodynamics, 3rd ed. (John Wiley & Sons, New York, 2007).
[25] I. Simonsen and A. A. Maradudin, Opt. Commun. **162**, 99 (1999).
[26] A. Madrazo and A. Maradudin, Opt. Commun. **134**, 251 (1997).
[27] K. ODonnell, C. West, and E. Méndez, Phys. Rev. B **57**, 13209 (1998).
[28] V. Agranovich and D. Mills (eds.), Surface Polaritons: ElectromagneticWaves at Surfaces and Interfaces, Modern Problems in Condensed Matter Science (North-Holland Publishing Company, Amsterdam, 1982).
[29] P. Johnson and R.W. Christy, Phys. Rev. B **6**, 4370 (1972).
[30] K. O'Donnell and E. Méndez, J. Opt. Soc. Am. A **20**, 2338 (2003).
[31] K. O'Donnell, J. Opt. Soc. Am. A **18**, 1507 (2001).